
Deep Sketched Output Kernel Regression for Structured Prediction

Tamim El Ahmad*



tamim.elahmad@telecom-paris.fr

Junjie Yang*



junjie.yang@telecom-paris.fr

Pierre Laforgue



pierre.laforgue@unimi.it

Florence d'Alché-Buc



florence.dalche@telecom-paris.fr

Abstract

By introducing a deep sketching layer in the output kernel regression framework, we propose a novel deep sketched output kernel regression (DSOKR) framework for structured prediction. The proposed framework is able to handle a wide range of structured prediction tasks, including text classification, image classification, and image captioning. The proposed framework is able to handle a wide range of structured prediction tasks, including text classification, image classification, and image captioning. The proposed framework is able to handle a wide range of structured prediction tasks, including text classification, image classification, and image captioning.

1 Introduction

Deep learning has achieved remarkable success in many domains, including image classification, text classification, and image captioning. However, deep learning is not well-suited for structured prediction tasks, where the output is a structured object (e.g., a sequence of labels, a set of labels, or a sequence of images). In this paper, we propose a novel deep sketched output kernel regression (DSOKR) framework for structured prediction. The proposed framework is able to handle a wide range of structured prediction tasks, including text classification, image classification, and image captioning. The proposed framework is able to handle a wide range of structured prediction tasks, including text classification, image classification, and image captioning. The proposed framework is able to handle a wide range of structured prediction tasks, including text classification, image classification, and image captioning.

¹EP

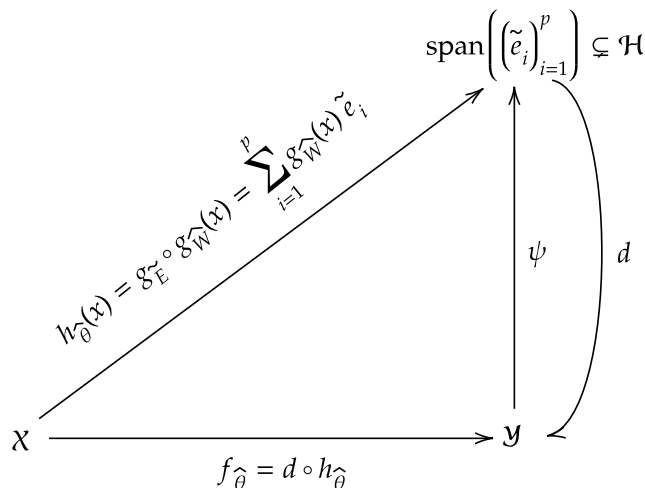


Fig: HDR

(Rasmussen, 2003; Cohn, 2005; Gauthier, 2006; Brundage, 2011, 2016; Spilhaus, 2016, 2020).

Output Kernel Regression. A function h is said to be \mathcal{H} -representable if there exist $n \geq 1$, $(y_i)_{i=1}^n \in \mathcal{Y}$, $(\alpha_i)_{i=1}^n \in \mathbb{R}^n$, and $\sum_{i,j=1}^n \alpha_i \alpha_j k(y_i, y_j) \geq 0$.
 The function h is \mathcal{H} -representable if and only if $\exists (y_i)_{i=1}^n \in \mathcal{Y}, (\alpha_i)_{i=1}^n \in \mathbb{R}^n, \sum_{i,j=1}^n \alpha_i \alpha_j k(y_i, y_j) \geq 0$ such that $h(y) = \sum_{i=1}^n \alpha_i k(y, y_i)$.
 Let $\mathcal{H} \subset \mathbb{R}^{\mathcal{Y}}$, $\psi: \mathcal{Y} \rightarrow \mathcal{H}$ be a mapping. Then $\Delta(y, y') := \|\psi(y) - \psi(y')\|_{\mathcal{H}}^2 = k(y, y) - 2k(y, y') + k(y', y')$.

$$\Delta(y, y') := \|\psi(y) - \psi(y')\|_{\mathcal{H}}^2 = k(y, y) - 2k(y, y') + k(y', y'). \quad (1)$$

Let \mathcal{H} be a Hilbert space. Then Δ is a positive semi-definite kernel on \mathcal{Y} . (Gauthier, 2008; Li, 2018; Brundage, 2020). Let \mathcal{H} be a Hilbert space. Then Δ is a positive semi-definite kernel on \mathcal{Y} . (Gauthier, 2008; Li, 2018; Brundage, 2020). Let \mathcal{H} be a Hilbert space. Then Δ is a positive semi-definite kernel on \mathcal{Y} . (Gauthier, 2008; Li, 2018; Brundage, 2020). Let \mathcal{H} be a Hilbert space. Then Δ is a positive semi-definite kernel on \mathcal{Y} . (Gauthier, 2008; Li, 2018; Brundage, 2020).

Let \mathcal{H} be a Hilbert space. Then Δ is a positive semi-definite kernel on \mathcal{Y} . Let \mathcal{H} be a Hilbert space. Then Δ is a positive semi-definite kernel on \mathcal{Y} . Let \mathcal{H} be a Hilbert space. Then Δ is a positive semi-definite kernel on \mathcal{Y} . Let \mathcal{H} be a Hilbert space. Then Δ is a positive semi-definite kernel on \mathcal{Y} .

$$\min_{\theta \in \Theta} \mathbb{E}_{(x,y) \sim \rho} [\|\psi(y) - \psi(f_{\theta}(x))\|_{\mathcal{H}}^2]. \quad (2)$$

Let ρ be a joint distribution on $\mathcal{X} \times \mathcal{Y}$. Let $\{(x_1, y_1), \dots, (x_n, y_n)\}$ be a sample from ρ . Let f_{θ} be a function from \mathcal{X} to \mathcal{Y} . Let ψ be a mapping from \mathcal{Y} to \mathcal{H} .

$$\hat{\theta} \in \arg \min_{\theta \in \Theta} L(\theta) = \arg \min_{\theta \in \Theta} \frac{1}{n} \sum_{i=1}^n \|h_{\theta}(x_i) - \psi(y_i)\|_{\mathcal{H}}^2, \quad (3)$$

Let $(h_\theta)_{\theta \in \Theta} \subset \mathcal{H}^{\mathcal{X}}$ be a family of functions.

\mathcal{H} .

$$f_{\hat{\theta}}(x) = \arg \min_{y \in \mathcal{Y}} \|h_{\hat{\theta}}(x) - \psi(y)\|_{\mathcal{H}}^2. \quad (4)$$

High-dimensional

\mathcal{H} and high-dimensional

is how can we design a neural architecture that is able to learn infinite-dimensional output kernel features?

Neural networks with infinite-dimensional outputs.

Let $p \geq 1$, $W \in \mathcal{W}$, $E = ((e_j)_{j=1}^p) \in \mathcal{H}^p$ functional and $g_E: \mathbb{R}^p \rightarrow \mathcal{H}$.

$$\theta = (W, E), \quad x \in \mathcal{X}, \quad h_\theta(x) := g_E \circ g_W(x), \quad (5)$$

Let g_W be

$L - 1$ layers

g_E function

$$E = (e_j)_{j=1}^p \in \mathcal{H}^p$$

$$g_E: z \in \mathbb{R}^p \mapsto \sum_{j=1}^p z_j e_j \in \mathcal{H}. \quad (6)$$

Non-pairwise dependence

Remark 1 (Peters et al., 2017)

\mathcal{H} .

g_W function

2.1 Learning neural networks with infinite-dimensional outputs

High

h_θ function

$\theta = (W, E)$.

Let $(\psi(y_i))_{i=1}^n$ be a sequence

E function

in \mathcal{H} .

Let $(x_i, \psi(y_i))_{i=1}^n$.

Estimating the functional last unit g_E . A possible

E function

is $\psi(y_j)_{j=1}^n$.

$p = n$ function

Anderson et al. (2019)

1997). Given

$$\mathcal{Y}, \quad C = \mathbb{E}_y[\psi(y) \otimes \psi(y)]$$

Let

$$\hat{C} = (1/n) \sum_{i=1}^n \psi(y_i) \otimes \psi(y_i)$$

S b

Let

$$f \in \mathcal{H} \quad (1/\sqrt{n})(f(x_1), \dots, f(x_n))^T$$

in \mathbb{R}^n , let

$S^\#$ function

$$S^\#: \alpha \in \mathbb{R}^n \mapsto (1/\sqrt{n}) \sum_{i=1}^n \alpha_i \psi(y_i) \in \mathcal{H},$$

Let

$$\hat{C} = S^\# S.$$

\hat{C} function

Let

$O(n^3)$.

capacity condition (Chen, 2020; El Aïme, 2024), i.e.

Let

$$\hat{C} \text{ (Chen, 2011),}$$

Let

Sketching for kernel methods. (Györfi, 2014)

Let

n function

Let $R \in \mathbb{R}^{m \times n}$, $m \ll n$. (El Ahmad et al., 2024), (Ghahramani, 2017), (Ghahramani et al., 2022).

Let $\mathcal{H}_Y = \text{span}((\sum_{j=1}^n R_{ij} \psi(y_j))_{i=1}^m)$. $R \in \mathbb{R}^{m \times n}$, $\mathcal{H} \subseteq \mathbb{R}^m$.

Sketching to estimate g_E .

Let $R \in \mathbb{R}^{m \times n}$. $\tilde{K} = RKR^T \in \mathbb{R}^{m \times m}$. $\tilde{E} \in \mathbb{R}^m$, $\tilde{\mathcal{H}}_Y \subseteq \mathcal{H}$. $p = \text{rank}(\tilde{K})$.

Proposition 1. (El Ahmad et al., 2024, Proposition 2) The eigenfunctions of the sketched empirical covariance operator $\tilde{C} = S^\# R^T R S$ are the $\tilde{e}_j = \sqrt{\frac{n}{\sigma_j(\tilde{K})}} S^\# R^T \tilde{\mathbf{v}}_j \in \mathcal{H}$, for $j \leq p$.

Let $\tilde{C} \in \mathbb{R}^{m \times m}$. $\mathcal{H} \subseteq \mathbb{R}^m$. $p \leq m$. $i = 1, \dots, m$.

$$f_i = \arg \max_{f \in \mathcal{H}} \{ \langle f, \tilde{C} f \rangle_{\mathcal{H}} : f \in \tilde{\mathcal{H}}_Y, \|f\|_{\mathcal{H}} = 1, f \perp \{f_1, \dots, f_{i-1}\} \} \quad (7)$$

Let $\tilde{\mathcal{H}}_Y = \text{span}((\sum_{j=1}^n R_{ij} \psi(y_j))_{i=1}^m)$. $\tilde{P} \in \mathbb{R}^{m \times m}$. $\tilde{C} = \tilde{P} \tilde{C} \tilde{P}$. $\tilde{K} = R^T \tilde{C} R$.

Remark 2. (El Ahmad et al., 2024, Proposition 2). (El Ahmad et al., 2024, Proposition 2). (El Ahmad et al., 2024, Proposition 2).

Learning the input neural network g_W . Let $\tilde{E} = (\tilde{e}_j)_{j \leq p}$.

Proposition 2. Given the pre-trained basis $\tilde{E} = (\tilde{e}_j)_{j \leq p}$, $L(\tilde{E}, W)$ expresses as

$$L(\tilde{E}, W) = \frac{1}{n} \sum_{i=1}^n \left\| g_W(x_i) - \tilde{\psi}(y_i) \right\|_2^2, \quad (8)$$

where $\tilde{\psi}(y) = (\tilde{e}_1(y), \dots, \tilde{e}_p(y))^T = \tilde{D}_p^{-1/2} \tilde{V}_p^T R k^y \in \mathbb{R}^p$, $\tilde{V}_p = (\tilde{\mathbf{v}}_1, \dots, \tilde{\mathbf{v}}_p)$, $\tilde{D}_p = \text{diag}(\sigma_1(\tilde{K}), \dots, \sigma_p(\tilde{K}))$, and $k^y = (k(y, y_1), \dots, k(y, y_n))$.

$$g_W = \min_{W \in \mathcal{W}} \frac{1}{n} \sum_{i=1}^n \left\| g_W(x_i) - \tilde{\psi}(y_i) \right\|_2^2. \quad (9)$$

Algorithm 1

input: $\{(x_i, y_i)\}_{i=1}^n, \{(y_i^c)\}_{i=1}^{n_c}, \{(x_i^{\text{val}}, y_i^{\text{val}})\}_{i=1}^{n_{\text{val}}}, \{(x_i^{\text{te}}, y_i^{\text{te}})\}_{i=1}^{n_{\text{te}}}, \mathbf{R} \in \mathbb{R}^{m \times n}, \mathbf{g}_W$
init: $\tilde{\mathbf{K}} = \mathbf{R} \mathbf{K} \mathbf{R}^\top \in \mathbb{R}^{m \times m}, \mathbf{K} = (k(y_i, y_j))_{1 \leq i, j \leq n} \in \mathbb{R}^{n \times n}$
// 1. a. Training of g_E : computations for the basis \tilde{E}
• $\tilde{\mathbf{D}}_p \in \mathbb{R}^{p \times p}, \tilde{\mathbf{V}}_p \in \mathbb{R}^{m \times p}, \tilde{\mathbf{V}}_p \tilde{\mathbf{D}}_p \tilde{\mathbf{V}}_p^\top = \tilde{\mathbf{K}}_p$
• $\tilde{\mathbf{\Omega}} = \tilde{\mathbf{D}}_p^{-1/2} \tilde{\mathbf{V}}_p^\top \in \mathbb{R}^{p \times m}$
// 1. b. Training of g_W : solving the surrogate problem
• $\tilde{\psi}(y_i) = \tilde{\mathbf{\Omega}} \mathbf{R} k^{y_i} \in \mathbb{R}^p, \forall 1 \leq i \leq n, \tilde{\psi}(y_i^{\text{val}}) = \tilde{\mathbf{\Omega}} \mathbf{R} k^{y_i^{\text{val}}} \in \mathbb{R}^p, \forall 1 \leq i \leq n_{\text{val}}$
• $\tilde{W} = \arg \min_{W \in \mathcal{W}} \frac{1}{n} \sum_{i=1}^n \|g_W(x_i) - \tilde{\psi}(y_i)\|_2^2$
• $\{(x_i^{\text{val}}, \tilde{\psi}(y_i^{\text{val}}))\}_{i=1}^{n_{\text{val}}}$
// 2. Inference
• $\tilde{\psi}(y_i^c) = \tilde{\mathbf{\Omega}} \mathbf{R} k^{y_i^c} \in \mathbb{R}^p, \forall 1 \leq i \leq n_c$
• $f_{\hat{\theta}}(x_i^{\text{te}}) = y_j^c, j = \arg \max_{1 \leq j \leq n_c} g_{\tilde{W}}(x_i^{\text{te}})^\top \tilde{\psi}(y_j^c), \forall 1 \leq i \leq n_{\text{te}}$
return $f_{\hat{\theta}}(x_i^{\text{te}}), \forall 1 \leq i \leq n_{\text{te}}$

A (3), (9) $h_{\theta} \in \mathcal{H}$ $W, C_{\hat{\theta}}$ \hat{C}, \tilde{C}, F
E), $m \geq p$ \mathcal{H}
Remark 3 (B) $\Delta(y, y') = c(\| \psi(y) - \psi(y') \|_{\mathcal{H}}^2), c: \mathbb{R}_+ \rightarrow \mathbb{R}_+$
 c (Ch 2020; Hb 1964; Ch 2008). $g_W \circ g_E, c$

2.2 The pre-image problem at inference time

Suppose in

$$d \circ h_{\hat{\theta}}(x) = \arg \min_{y \in \mathcal{Y}} k(y, x) - 2g_{\tilde{W}}(x)^\top \tilde{\psi}(y) = \arg \max_{y \in \mathcal{Y}} g_{\tilde{W}}(x)^\top \tilde{\psi}(y)$$

For k $k(y, y') = 1, \forall y, y' \in \mathcal{Y}$. For $X^{\text{te}} = (x_1^{\text{te}}, \dots, x_{n_{\text{te}}}^{\text{te}}) \in \mathcal{X}^{n_{\text{te}}}$ $Y^c = (y_1^c, \dots, y_{n_c}^c) \in \mathcal{Y}^{n_c}, 1 \leq i \leq n_{\text{te}}, 1 \leq j \leq n_c$

$$f_{\hat{\theta}}(x_i^{\text{te}}) = y_j^c, j = \arg \max_{1 \leq j \leq n_c} g_{\tilde{W}}(x_i^{\text{te}})^\top \tilde{\psi}(y_j^c). \quad (10)$$

He $\psi(y)$ $\psi(y')$ \mathcal{H}
 (2007) \mathcal{H} (2018) \mathcal{H}
 \mathcal{H}

3 Experiments

He $\psi(y)$ $\psi(y')$ \mathcal{H}
 \mathcal{H}

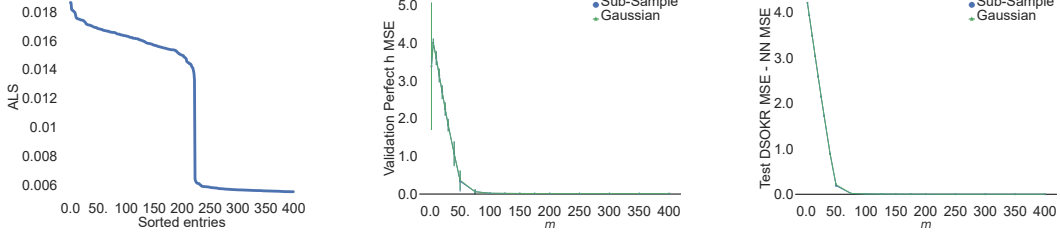


Fig. 2: 6400 GAT, M6
 DSOKR

Perfect h w m (h)

Perfect h w m (h)

Sketching size selection strategy. A

Perfect h w m (h)

Perfect h w m (h)

Perfect h w m (h)

Perfect h w m (h)

$$h_\psi(x) = \sum_{j=1}^p \langle \tilde{e}_j, \psi(y) \rangle_{\mathcal{H}} \tilde{e}_j = \sum_{j=1}^p \tilde{\psi}(y)_j \tilde{e}_j. \quad (11)$$

Perfect h w m (h)

Perfect h w m (h)

3.1 Analysis of DSOKR on Synthetic Least Squares Regression

Dataset. Perfect h w m (h)

Perfect h w m (h)

Perfect h w m (h)

Perfect h w m (h)

Perfect h w m (h)

Perfect h w m (h)

Perfect h w m (h)

$$y_i = UHx_i + \varepsilon_i, \quad (12)$$

Perfect h w m (h)

Perfect h w m (h)

Experimental settings. Perfect h w m (h)

Perfect h w m (h)

Perfect h w m (h)

Perfect h w m (h)

Perfect h w m (h)

$$h_{\hat{\theta}}(x) = Y^T R^T \tilde{V}_p \tilde{D}_p^{-1/2} g_{\tilde{W}}(x). \quad (13)$$

Perfect h w m (h)

Perfect h w m (h)

Enthalpy (kcal/mol) vs. Entropy (kcal/mol) plot for the ADAM dataset (Ba2015). The plot shows Perfect h (red) and m (blue) curves. The x-axis ranges from 0 to 400, and the y-axis ranges from 0 to 100. The m curve is a straight line, and the Perfect h curve is a curve that starts at (0,0) and increases towards (400,100). The plot is labeled with $m \in [2, 400]$.

Experimental results. Fig. 1 shows the performance of the model on the ADAM dataset (Ba2015) for $d = 50$. The plot shows Perfect h (red) and m (blue) curves. The x-axis ranges from 0 to 400, and the y-axis ranges from 0 to 100. The m curve is a straight line, and the Perfect h curve is a curve that starts at (0,0) and increases towards (400,100). The plot is labeled with $m = 75$, $d = 50$, and ϵ_i . The plot is also labeled with $m = 75$ and $150,075$.

3.2 SMILES to Molecule: SMI2Mol

Dataset. (MolScribe, 2012; Li, 2014), containing 30,000 molecules. The dataset is split into training (80%), validation (10%), and test (10%) sets. The training set is used for training the model, the validation set is used for monitoring the performance, and the test set is used for evaluating the performance. The dataset is labeled with SMI2Mol.

Experimental set-up. The model is trained on the SMI2Mol dataset for 13,382 steps (500 epochs) with a learning rate of $1e-4$ (Schuett, 2017). The model is evaluated on the validation set (10%) and the test set (10%). The performance is measured by the Perfect h (red) and m (blue) curves. The plot is labeled with m and ϵ_i . The plot is also labeled with $m = 75$ and $150,075$.

Experimental results. Fig. 2 shows the performance of the model on the SMI2Mol dataset for $d = 50$. The plot shows Perfect h (red) and m (blue) curves. The x-axis ranges from 0 to 400, and the y-axis ranges from 0 to 100. The m curve is a straight line, and the Perfect h curve is a curve that starts at (0,0) and increases towards (400,100). The plot is labeled with $m = 75$ and $150,075$.

¹RKCh

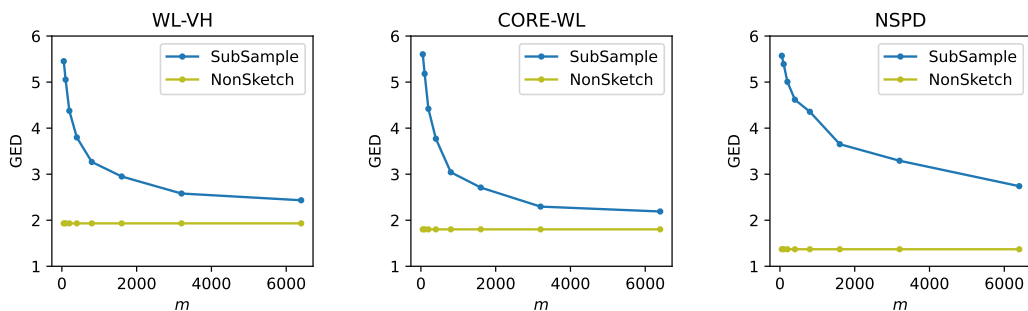


Fig: GED vs m for the BM method. $m > 6400$

m to Perfect h

EF: E

	GED w/o EF	↓	GED w/ EF	↓
R	3.330 ± 0.080		4.192 ± 0.109	
R -FGW	5.115 ± 0.129		-	
E -FGW	2.998 ± 0.253		-	
D R	1.951 ± 0.074		2.960 ± 0.079	

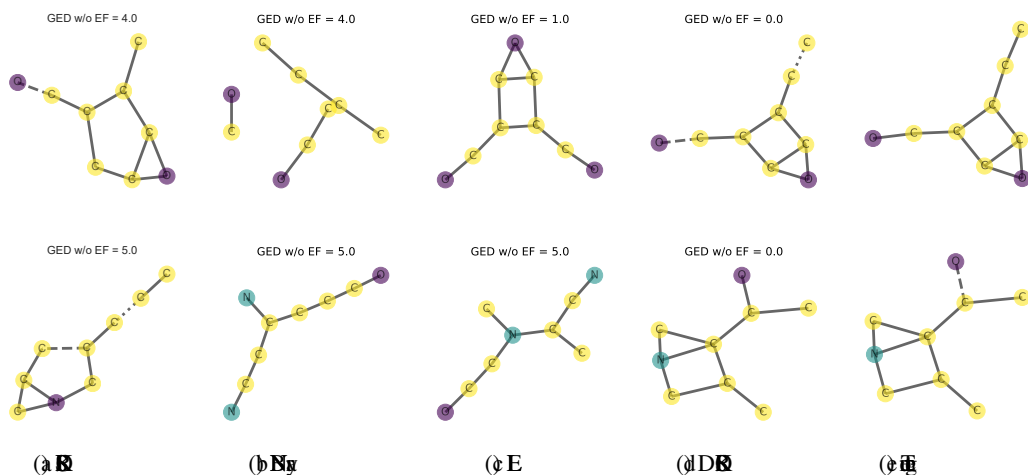


Fig: E

3.3 Text to Molecule: ChEBI-20

Dataset. ChEBI20 (Eich, 2021) consists of 33,010 pairs of SMILES and text (Eich et al., 2016, 2019), split into 20 ChEBI (CEB) classes (Eich, 2016). 80% of the data is used for training, 10% for validation, and 10% for testing. The dataset is available at <https://github.com/cheminformatics/cheminformatics>.

Experimental set-up. For the evaluation, we use the setup from (Eich, 2018) with a maximum length of 256. The evaluation is performed on 1000 samples.

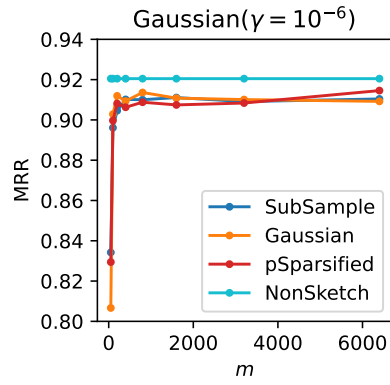
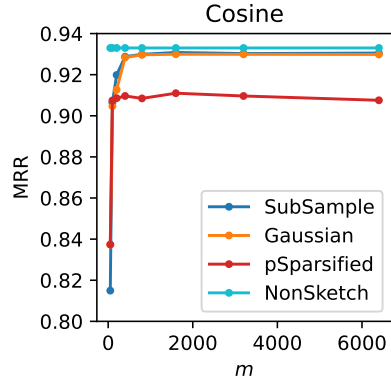


Fig. 5: MRR on CEBI20 dataset

m 6 Perfect h

Fig. 6: MRR on CEBI20 dataset

		H@1 ↑	H@10 ↑	RI ↑	
BE		0.4%	2.8%	0.015	
BE		16.8%	56.9%	0.298	

CMM		34.9%	84.2%	0.513	
CMMGCN		33.2%	82.5%	0.495	
CMMEM	×3)		39.8%	87.6%	0.562
CMMEMGCN	×3)		39.0%	87.0%	0.551
CMMEM	×3 + GCN×3)		44.2%	88.7%	0.597
DR		48.2%	87.4%	0.624	
DRGa		49.0%	87.5%	0.630	
DRER	×3)		51.0%	88.2%	0.642
DRERGa	×3)		50.5%	87.9%	0.642
DRER	×3 + Ga	×3)	50.0%	88.3%	0.640

Fig. 7: Performance of different methods on CEBI20 dataset. The methods are compared based on H@1, H@10, and RI. The best performance is achieved by DRER (×3 + Ga) with H@1 of 50.0%, H@10 of 88.3%, and RI of 0.640.

{10⁻⁹, 10⁻⁶, 10⁻³, 1},

Perfect h

²<https://github.com/cnedwards/text2mol>

Ensemble. [Fisch \(2021\)](#), [Hartsh](#)

R_t t , $1 \leq t \leq T$,

$$s(y_i) = \sum_{t=1}^T w_t R_t(y_i) \quad \text{s.t.} \quad \sum_{i=1}^T \omega_t = 1 \quad (14)$$

in y_i R_t

R_t R_t g_{W_t}

g_{W_t} x y ,

$$s(x, y) = \sum_{t=1}^T \omega_t g_{W_t}(x)^\top \tilde{\psi}_t(y) \quad \text{or} \quad s(x, y) = \arg \max_{1 \leq t \leq T} g_{W_t}(x)^\top \tilde{\psi}_t(y). \quad (15)$$

R_t

Experimental results. [Fig 1](#)

$\gamma = 10^{-6}$

$m = 100, 300$

$m = 100, 300$

$m = 100, 300$

$m = 100, 300$

$m = 100, 300$

$m = 100, 300$

$m = 100, 300$

$m = 100, 300$

$m = 100, 300$

4 Conclusion

$m = 100, 300$

$m = 100, 300$

$m = 100, 300$

$m = 100, 300$

Acknowledgments and Disclosure of Funding

$m = 100, 300$

$m = 100, 300$

$m = 100, 300$

$m = 100, 300$

01120237 (EAS)

Af

FR

References

A.A. (2015). [Fisch](#)

[ICML](#), [NIPS](#), [ICML](#)

in *Neural Information Processing Systems (NeurIPS)*, 18.

Advances

B.F. (2013). [Fisch](#)

annual *Conference on Learning Theory*, 185209. [ML](#)

Proc. of the 26th

- Berg, Herta, J. B., et al. (2007). *Predicting structured data*.
- Berg, D., et al. (2016). *International Conference on Machine Learning*, 839-92.
- Berg, D., et al. (2017). *Proceedings of the 34th International Conference on Machine Learning, Proceedings of Machine Learning Research*, 4294-39.
- Berg, D., et al. (2019). *Proceedings of the 2019 Conference on Empirical Methods in Natural Language Processing and the 9th International Joint Conference on Natural Language Processing (EMNLP-IJCNLP)*, 6153-620.
- Berg, D., et al. (2020). *Foundations and Trends in Machine Learning*, 13(5-6):531-712.
- Berg, D. (2005). *Fifth IEEE International Conference on Data Mining (ICDM'05)*, 8-16.
- Berg, D., et al. (2022). *Proceedings of the 39th International Conference on Machine Learning, Proceedings of Machine Learning Research*, 3212-335.
- Berg, D., et al. (2011). *International Conference on Machine Learning (ICML)*, 593-600.
- Berg, D., et al. (2016). *Bioinformatics*, 32(12):2836.
- Berg, D., et al. (2016). *The Journal of Machine Learning Research*, 17(1):6105-6152.
- Chen, B., et al. (2021). *conference on learning theory*, 2386-5.
- Chen, B., et al. (2016). *Advances in Neural Information Processing Systems (NIPS)* 29, 4124-420.
- Chen, B., et al. (2020). *J. Mach. Learn. Res.*, 21(98):167.
- Chen, B. (2005). *International Conference on Machine Learning (ICML)*, 53-60.
- Chen, B. (2007). *Predicting Structured Data*.
- Chen, B. (2010). *Proceedings of the 27th International Conference on International Conference on Machine Learning, CM0*, 552-62.
- Chen, B., et al. (2019). *Proceedings of the Twenty-Eighth International Joint Conference on Artificial Intelligence (IJCAI-19)*.
- Chen, B. (2005). *JMLR*, 6(12).

- EdC., ZC., dJ H. (2021). *Proceedings of the 2021 Conference on Empirical Methods in Natural Language Processing*, 95607, 95607.
- ElAHT BgM, dP dA BgF. (2024). *Proceedings of The 27th International Conference on Artificial Intelligence and Statistics*, 109417. *Proceedings of Machine Learning Research*, 9
- ElAHT BgM, dP dA BgF. (2023). *Transactions on Machine Learning Research*.
- Gd T(2008). *Kernels for Structured Data*, 626. *Series in Machine Perception and Artificial Intelligence*.
- Gd P, dA BgF. (2006). *Proceedings of the 23rd International Conference on Machine Learning*, 345352, 345352. *ICML*
- Gd C., dM dA. (2018). *Advances in Neural Information Processing Systems*, 31.
- Gd M, dM dA. (2017). *Proceedings of the 34th International Conference on Machine Learning - Volume 70*, 3414351. *ICML*
- Hg A. A., dD. A., dP (2008). *Proceedings of the 7th Python in Science Conference*, 1-15, *SCA*.
- Hg J, dG., dK A., dM K, dM S. *Nucleic Acids Research*, 44(D1):D1214-D1219.
- Hg P (1964). *The Annals of Mathematical Statistics*, 73401.
- J S Fh S dS (2018). *Journal of Chemical Information and Modeling*, 58(1):2735.
- J, dE R P A., dG T F dC. *Nature*, 596(7873):583589.
- KH., dM dP (2013). *International Conference on Machine Learning (ICML)*, 471479.
- KS Ch J, dT G dA., He J, He S L Q dB. A., dP A., dM B., dL, dJ, dM E. E. (2019). *Nucleic Acids Research*, 47(D1):D1102-D1109.
- KS dP A., dM E. E., Ch J, Fu G., G dA., Ha L, He J, He S dB. A., dM B., dL, dM SH. (2016). *Nucleic Acids Research*, 44(D1):D1202-D1213.
- dD. dP dA J (2015). *3rd International Conference on Learning Representations, ICLR 2015, San Diego, CA, USA, May 7-9, 2015, Conference Track Proceedings*.
- K A., dM E., dM M H., dC., dG L, dT M S Bg A. C., dM Y d (2023). *Proceedings of the IEEE/CVF International Conference on Computer Vision*, 40154026.

K.A., G.A., and A.B.F. (2018). A paper in *Advances in Neural Information Processing Systems*, 31.

K.S.B. K(2020). A paper in *AISTATS 2020, Proceedings of Machine Learning Research*, 9283937.

J.M(2022). A paper in *IEEE Transactions on Information Theory*, 68(5):32813303.

P.A., B.M., and A.B.F. (2020). A paper in *International Conference on Machine Learning*, 5985607.

E.Y.C.S.H.R.A., and H.F. J(2006). A paper in *Predicting structured data*.

J.Y.D., G.P.Z.W.Z., and A. (2022). A paper in *Advances in Neural Information Processing Systems*.

L.Z.F., D., and D. (2021). A paper in *Journal of Machine Learning Research*, 22(108):151.

M. (2011). A paper in *Foundations and Trends in Machine Learning*, 3(2):123224.

G., C.L.R., and A. (2020). A paper in *Advances in Neural Information Processing Systems (NeurIPS)*, 33.

G., C.A., K.R.P., and R.L(2023). A paper in *Thirty-seventh Conference on Neural Information Processing Systems*.

G., P.S., and M(2018). A paper in *Proceedings of the Twenty-Seventh International Joint Conference on Artificial Intelligence, IJCAI-18*, 25952601.

A., B.F., and A. (2019). A paper in *Proceedings of the Twenty-Second International Conference on Artificial Intelligence and Statistics (AISTATS), Proceedings of Machine Learning Research*, 9204929.

A., B.F., and A. (2020). A paper in *Proceedings of the 37th International Conference on Machine Learning, Proceedings of Machine Learning Research*, 3817391.

S.C. H. (2011). A paper in *Foundations and Trends in Computer Graphics and Vision*, 6(3-4):185365.

A. B. (2007). A paper in *NIPS*, 20:1177–1184.

R.L., S.J., S.H., and B.P(2005). A paper in *Neural Networks*, 18(8):10934110.

R.D., P.O., and M.L.O.A. (2014). A paper in *Scientific Data*, 1.

- BL, DR, BL, C., et al. (2012). Efficient Graph Neural Network for Graph Classification. *Journal of Chemical Information and Modeling*, 52(11):2864-2875.
- BA., CA, RL (2015). Advances in Neural Information Processing Systems, 28.
- BA., RL (2017). Advances on Neural Information Processing Systems (NeurIPS), 30:2153-2225.
- SB., HA., VKR (1997). International conference on Artificial Neural Networks (ICANN), 8:583-588.
- SB. (1983). *Social Networks*, 5(3):269-287.
- NEP, E. J., K, B, G, M (2011). *Journal of Machine Learning Research*, 12(77):2539-2561.
- SG., NG., S, G, C., K, G, M (2020). *Journal of Machine Learning Research*, 21(54):15.
- LI, CHA. (2008). Advances in Neural Information Processing Systems 21 (NeurIPS), 1:569-576.
- SNBB., RL, BA. (2020). Proceedings of the Twenty Third International Conference on Artificial Intelligence and Statistics, 1:808-816. *Proceedings of Machine Learning Research*, 164:236-252.
- SNBB. K (2022). *Journal of Machine Learning Research*, 23(337):132.
- FI (1958). *An Elementary Mathematical Theory of Classification and Prediction*.
- PA., BUS, S, H, M (2023). *Thirty-seventh Conference on Neural Information Processing Systems*.
- IL, G, K (2018). *International Conference on Learning Representations*.
- VA., N, N, W, J, L, G, A, N, K, L, d (2017). *Advances in Neural Information Processing Systems (NIPS)*, 30:9986-6008.
- AT, C, N, R, L, C., d, F, R (2019). *Proceedings of the 36th International Conference on Machine Learning*, 1:76-87. *Proceedings of Machine Learning Research*, 139:2756-284.
- SB. HA. (1968). *Journal of Machine Learning Research*, 2(9):12-16.
- W, C, O, W, E, E, A., d, S, B. (2003). *Advances in Neural Information Processing Systems 15*, 9:979-904.
- MC. SM (2001). *Advances in Neural Information Processing Systems*, 14:826-888.
- WD. P (2014). *Found. Trends Theor. Comput. Sci.*, 10(1-2):14-57.

1. TL; MR; ZH. (2012). *Advances in Neural Information Processing Systems*, 25.

2. A; F; C. J. C., B; L. (2017). *The Annals of Statistics*, 45(3):991-1023.

3. D., C; B., K; C; J. (2024). *IEEE Transactions on Artificial Intelligence*, 5(1):278-289.

A Technical proof

Prop.

Proposition 2. Given the pre-trained basis $\tilde{E} = (\tilde{e}_j)_{j \leq p}$, $L(\tilde{E}, W)$ expresses as

$$L(\tilde{E}, W) = \frac{1}{n} \sum_{i=1}^n \left\| g_W(x_i) - \tilde{\psi}(y_i) \right\|_2^2, \quad (8)$$

where $\tilde{\psi}(y) = (\tilde{e}_1(y), \dots, \tilde{e}_p(y))^\top = \tilde{D}_p^{-1/2} \tilde{V}_p^\top \mathbf{R} \mathbf{k}^y \in \mathbb{R}^p$, $\tilde{V}_p = (\tilde{\mathbf{v}}_1, \dots, \tilde{\mathbf{v}}_p)$, $\tilde{D}_p = \text{diag}(\sigma_1(\tilde{\mathbf{K}}), \dots, \sigma_p(\tilde{\mathbf{K}}))$, and $\mathbf{k}^y = (\mathbf{k}(y, y_1), \dots, \mathbf{k}(y, y_n))$.

Proof. For $(x, y) \in \mathcal{X} \times \mathcal{Y}$,

$$\begin{aligned} \|h_\theta(x) - \psi(y)\|_{\mathcal{H}}^2 &= \left\| \sum_{i=1}^p g_W(x)_i \tilde{e}_i - \psi(y) \right\|_{\mathcal{H}}^2 \\ &= \sum_{i,j=1}^p g_W(x)_i g_W(x)_j \langle \tilde{e}_i, \tilde{e}_j \rangle_{\mathcal{H}} - 2 \sum_{j=1}^p g_W(x)_j \langle \tilde{e}_j, \psi(y) \rangle_{\mathcal{H}} + k(y, y) \\ &= \|g_W(x)\|_2^2 - 2g_W(x)^\top \tilde{\psi}(y) + k(y, y), \end{aligned}$$

$$\tilde{E} \text{ is orthonormal} \quad \langle \tilde{e}_j, \psi(y) \rangle_{\mathcal{H}} = \tilde{e}_j(y) = \tilde{\psi}(y)_j$$

$$\left\| g_W(x) - \tilde{\psi}(y) \right\|_2^2 = \|g_W(x)\|_2^2 - 2g_W(x)^\top \tilde{\psi}(y) + \left\| \tilde{\psi}(y) \right\|_2^2, \quad (16)$$

$$\text{and } k(y, y) = \left\| \tilde{\psi}(y) \right\|_2^2 \quad \square$$

B Graph Prediction via Output Kernel Regression

Notation.

A graph $G = (V, E)$ with vertex set V and edge set E . E is a subset of $\binom{V}{2}$.

Fingerprints.

(Schölkopf et al., 2005;

Borgwardt et al., 2016; Feng et al., 2023). A fingerprint

$$d \geq 1$$

is a function $f: V \rightarrow \mathbb{R}^d$.

Let H_d be the Hilbert space

of functions $f: V \rightarrow \mathbb{R}^d$.

(Schölkopf et al., 1998), with inner

product

Graph kernels.

(Schölkopf et al., 2005;

Foster et al., 2020).

Definition 1 (Foster

et al., 2020). Let $\mathcal{L} = \{1, \dots, d\}$ and

let $G = (V, E)$ and $G' = (V', E')$ be

graphs with $\ell: v \in V \mapsto \ell(v) \in \mathcal{L}$.

Let

$$f = (f_1, \dots, f_d)^\top,$$

where $f_i = |\{v \in V : \ell(v) = i\}|$ and $i \in \mathcal{L}$. Let f, f' be

functions $f, f': \mathcal{L} \rightarrow \mathbb{R}$.

$$G, G',$$

then

$$f \text{ and } f',$$

$$k(G, G') = f^\top f'. \quad (17)$$

Lemma 1

(Foster et al., 2020)

Definition 2 (Bok 2005) Let $G = (V, E)$ and $G' = (V', E')$ be graphs such that $S = (V, E_S)$ and $S' = (V', E'_{S'})$ are subgraphs of G and G' respectively, with $E_S \subseteq E$ and $E'_{S'} \subseteq E'$.

$$k(G, G') = k(S, S') = \sum_{e \in E} \sum_{e' \in E'} k_{\text{walk}}^{(1)}(e, e'), \quad (18)$$

where $k_{\text{walk}}^{(1)}(e, e')$ is the number of walks of length 1 from e to e' .

The complexity of computing $k_{\text{walk}}^{(1)}$ is $\mathcal{O}(n_V)$ for each pair of edges (e, e') , where n_V is the number of vertices.

(Cai and Gu 2010).

Definition 3 (Cai and Gu 2010) Let $G = (V, E)$ and $G' = (V', E')$ be graphs. For $u, v \in V$, $D(u, v)$ is the distance between u and v , i.e., the length of the shortest path between u and v . Let $r \geq 1$ be an integer. Define $S_r = \{u \in V : D(u, v) \leq r\}$ as the r -neighborhood of v . Let $A_v, B_u \in \{N_r^v : v \in V\}$ be two neighborhoods. Let $R_{r,d}(A_v, B_u, G)$ be the set of edges (A_v, B_u) in $R^{-1}(G)$ such that $D(u, v) = d$.

$$k_{r,d}(G, G') = \sum_{A_v, B_u \in R_{r,d}^{-1}(G)} \sum_{A_{v'}, B_{u'} \in R_{r,d}^{-1}(G')} \delta(A_v, A_{v'}) \delta(B_u, B_{u'}), \quad (19)$$

where δ is the Kronecker delta function, $\delta(x, y) = 1$ if $x = y$ and 0 otherwise.

$$k(G, G') = \sum_{r=0}^{r^*} \sum_{d=0}^{d^*} \hat{k}_{r,d}(G, G'), \quad (20)$$

where $\hat{k}_{r,d}$ is the (r, d) -th component of the distance matrix.

The complexity of computing $\hat{k}_{r,d}$ is $\mathcal{O}(n_V^2)$.

(Cai and Gu 1968), where h is the number of vertices.

Definition 4 (Cai 2011) Let $G = (V, E)$ and $G' = (V', E')$ be graphs. Let $\ell = \ell_0$ and $\ell' = \ell'_0$ be integers. Let G_i be the graph obtained from G by removing the i -th vertex. Let $k_{\text{base}}(G, G')$ be the base complexity of G and G' .

$$k(G, G') = k_{\text{base}}(G_0, G'_0) + \dots + k_{\text{base}}(G_h, G'_h). \quad (21)$$

The complexity of computing k_{base} is $\mathcal{O}(hn_E)$, where n_E is the number of edges.

with k -diffs (1983).

Definition 5 (Cohen, 2018)

Let $G_{\text{sub}}(S, E(S))$ be the subgraph of G induced by S .

k -diffs

Let $G = (V, E)$ and $G' = (V', E')$ be graphs with $S \subseteq V$ and

$S \subseteq V'$. Let $d_{G_{\text{sub}}}(v)$ be the degree of v in G_{sub} . Let C_k be the set of k -diffs between G and G' .

$$k(G, G') = k_{\text{base}}(C_0, C'_0) + \dots + k_{\text{base}}(C_{\delta_{\min}^*}, C'_{\delta_{\min}^*}), \quad (22)$$

where δ_{\min}^* is the minimum degree of C'_i .

G and G' .

$1 \leq i \leq \delta_{\min}^*, C_i$ and

Let $O(n_V + n_E)$.

k -diffs

$O(n_V + n_E)$.

C Additional Experimental Details

SMI2Mol

C.1 Additional Experimental Details for SMI2Mol

For SMI2Mol, we used a dataset of 50 molecules. The dataset was split into training and testing sets. The training set was used to train the model, and the testing set was used to evaluate the model. The results are shown in Table 1.

10^{-3}

$\{3, 6\}$, 8 , 0.2 .

$\{256, 512\}$, h

C.2 Additional Experimental Details for ChEBI-20

For ChEBI-20, we used a dataset of 50 molecules. The dataset was split into training and testing sets. The training set was used to train the model, and the testing set was used to evaluate the model. The results are shown in Table 1.

Fig. 6

γ is γ 10^{-6} *Perfect h* γ *Perfect h*.

ICM@1, 50%, γ
ICM@10, 88%, γ
with 2% γ

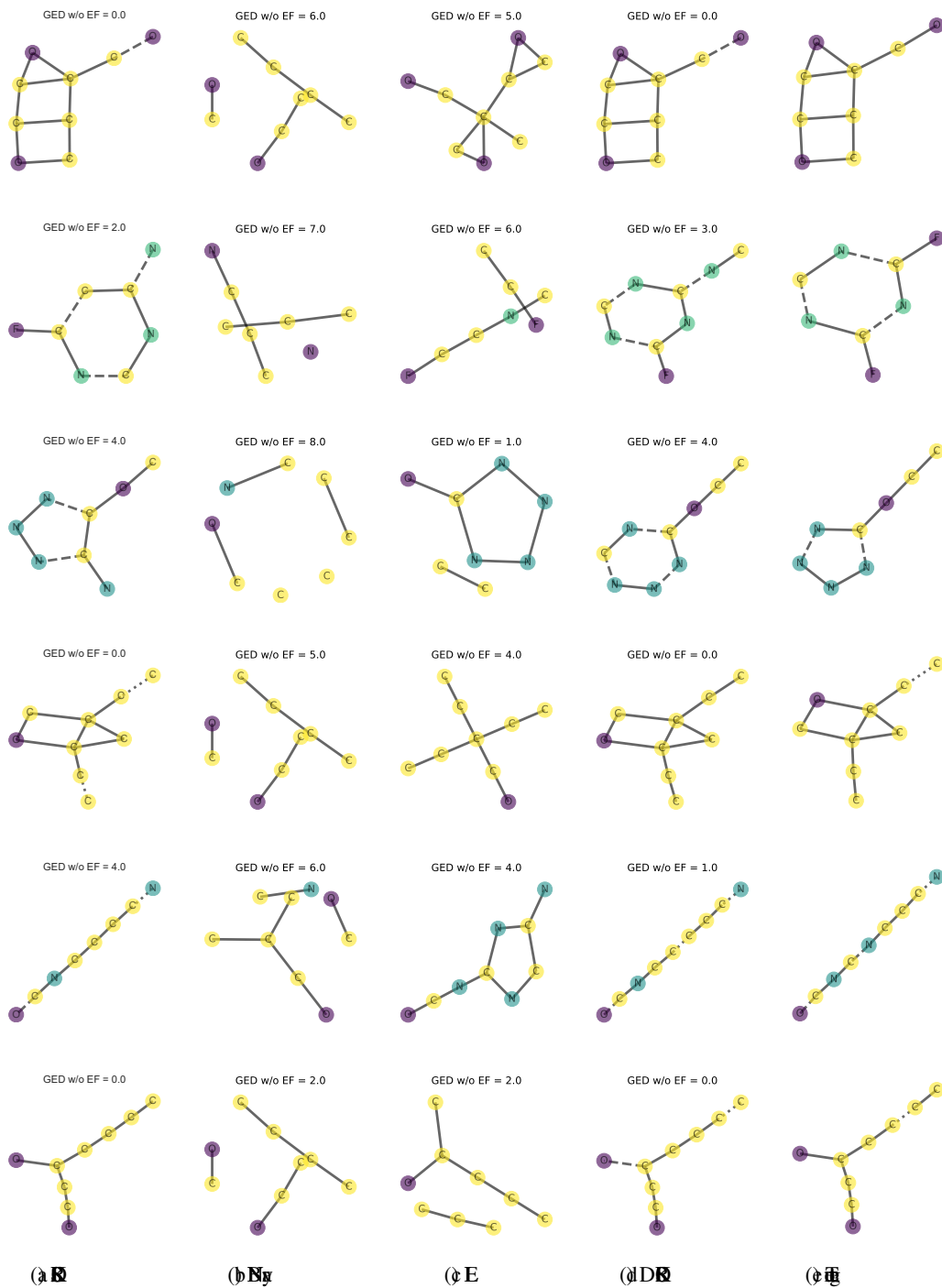


Fig: ~~10~~ **10**

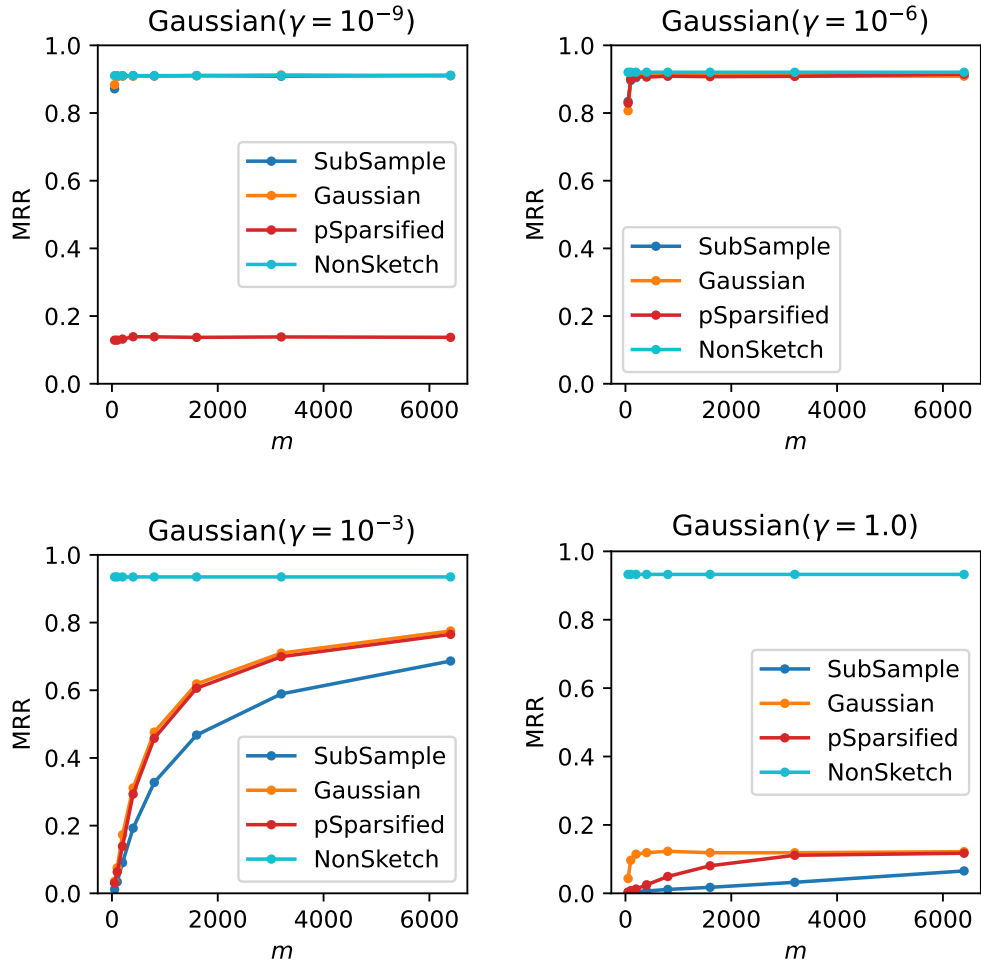


Fig: MICEBI20 to All

$\gamma \in \{10^{-9}, 10^{-6}, 10^{-3}, 1.0\}$.

Fig: MICEBI20 to All

	\mathcal{M}	$\downarrow \mathcal{R}$	$\uparrow \mathcal{H}@1$	$\uparrow \mathcal{H}@10$
R	2230.48	0.015	0.4%	2.8%
BER	344.53	0.298	16.8%	56.9%
<hr/>				
CM	23.74	0.513	34.9%	84.2%
CMGCN	24.11	0.495	33.2%	82.5%
CMEM	17.92	0.562	39.8%	87.6%
CMEMGCN	20.48	0.551	39.0%	87.0%
CMEMGCN		16.28	0.597	44.2%
<hr/>				
DE	82.92	0.624	48.2%	87.4%
DEG	91.19	0.630	49.0%	87.5%
DEK	76.43		0.642	51.0%
DEKG	81.70		0.642	50.5%
DEKGA	76.87	0.640	50.0%	88.3%